Acta Crystallographica Section D
Biological Crystallography
ISSN 0907-4449

DNA apophotolyase from *Anacystis nidulans*: 1.8 Å structure, 8-HDF reconstitution and X-ray-induced FAD reduction

Remco Kort,[a]* Hirofumi Komori,[b] Shin-ichi Adachi,[c] Kunio Miki[b,c] and Andre Eker[d]

[a]Laboratory for Microbiology, Swammerdam Institute for Life Sciences, University of Amsterdam, Nieuwe Achtergracht 166, 1018 WV Amsterdam, The Netherlands, [b]Department of Chemistry, Graduate School of Science, Kyoto University, Sakyo-ku, Kyoto 606-8502, Japan, [c]RIKEN Harima Institute/SPring-8, Koto 1-1-1, Mikazukicho, Sayo-gun, Hyogo 679-5148, Japan, and [d]MGC–Department of Cell Biology and Genetics, Erasmus University Medical Centre, PO Box 1738, 3000 DR Rotterdam, The Netherlands

Correspondence e-mail: rkort@science.uva.nl

Received 24 February 2004
Accepted 19 April 2004

PDB References: DNA photolyase, 1owl, r1owlsf; 1owm, r1owmsf; 1own, r1ownsf; 1owo, r1owosf; 1owp, r1owpsf.

DNA photolyase is a unique flavoenzyme that repairs UV-induced DNA lesions using the energy of visible light. *Anacystis nidulans* photolyase contains a light-harvesting chromophore, 8-hydroxy-5-deazaflavin (8-HDF), and flavin adenine dinucleotide (FAD) which, in contrast to the 8-HDF chromophore, is indispensable for catalytic activity. This work reports the crystallization and structure at 1.8 Å resolution of DNA photolyase devoid of its 8-HDF chromophore (apophotolyase). The overall three-dimensional structure is similar to that of the holoenzyme, indicating that the presence of 8-HDF is not essential for the correct folding of the enzyme. Structural changes include an additional phosphate group, a different conformation for Arg11 and slight rearrangements of Met47, Asp101 and Asp382, which replace part of the 8-HDF molecule in the chromophore-binding pocket. The apophotolyase can be efficiently reconstituted with synthetic 8-hydroxy-5-deazariboflavin, despite the orientation of Arg11 and the presence of the phosphate group in the 8-HDF pocket. Red light or X-rays reduced the FAD chromophore in apophotolyase crystals, as observed by single-crystal spectrophotometry. The structural effects of FAD reduction were determined by comparison of three data sets that were successively collected at 100 K, while the degree of reduction was monitored online by changes in the light absorption of the crystals. X-ray-induced conformational changes were confined to the active site of the protein. They include sub-ångström movements of the O(2) and N(5) atoms of the flavin group as well as the O^{δ} atoms of the surrounding amino acids Asp380 and Asn386.

1. Introduction

The UV component of solar radiation causes DNA damage, which is detrimental to the living cell as it interferes with the correct replication and transcription of DNA. The major products of UV irradiation of DNA are cyclobutane dimers formed between adjacent pyrimidine bases in the same DNA strand, which can be repaired by DNA photolyase. This enzyme utilizes light energy (300–500 nm) to split the cyclobutane ring of the dimer. DNA photolyase is a monomeric protein of approximately 50 kDa with stoichiometric amounts of two non-covalently bound chromophores. The first chromophore is $FADH^{-}$, which is essential for catalysis, while the second chromophore only plays a role in light-harvesting and can be either 5,10-methenyltetrahydrofolate (MTHF) or 8-hydroxy-5-deazaflavin (8-HDF). Two distinct photochemical reactions are mediated by DNA photolyase. The actual DNA-repair reaction, commonly referred to as photoreactivation,

Table 1
Data-collection and refinement statistics.

Values in parentheses are for the last resolution shell.

Data collection	DATA1†	DATA2†	DATA3†	DATA4‡	DATA5‡	DATA6‡	DATA7§
Resolution range (Å)	20.0–2.3	20.0–2.3	20.0–2.3	20.0–2.3	20.0–2.3	20.0–2.3	20.0–1.75
Resolution range, last shell (Å)	2.38–2.3	2.38–2.3	2.38–2.3	2.38–2.3	2.38–2.3	2.38–2.3	1.81–1.75
Total No. observations	114746	114879	115071	119038	118066	118365	305896
No. unique reflections	21712	21671	21636	21372	21264	21794	51041
Completeness $I > 1\sigma$ (%)	87.8 (73.6)	87.6 (73.6)	87.5 (72.4)	85.4 (68.6)	85.0 (66.7)	87.1 (70.4)	90.2 (79.2)
$R_{\rm merge}$¶ (%)	5.7 (22.6)	5.5 (23.1)	5.5 (23.2)	9.3 (27.3)	9.4 (29.2)	7.7 (23.2)	6.1 (39.0)
Unit-cell parameters							
$a = b$ (Å)	89.33			89.74			90.01
c (Å)	133.40			133.82			134.78
Refinement							
Resolution (Å)	20.0–2.3			20.0–2.3			20.0–1.80
R†† (%)	20.7			20.6			19.0
$R_{\rm free}$†† (%)	26.0			24.1			21.1
Model (No. atoms)	4067			4072			4255
Protein (No. residues)	474			474			475
Cofactor	FAD			FAD			FAD
Solvent molecules (waters/PO_4^{3-})	223/1			228/1			416/2‡‡
PDB code	1owm		1own	1owo		1owp	1owl

† Data were collected at beamline BL44B2, SPring-8 with monochromatic X-rays of 1.00 Å wavelength. The corresponding spectra recorded before each diffraction data-set collection are indicated in Fig. 4(*a*): DATA1, squares; DATA2, circles; DATA3, triangles. ‡ Data were collected from at beamline BL44B2, SPring-8 with monochromatic X-rays of 1.00 Å wavelength from a crystal devoid of the $FADH^{\cdot}$ state. The corresponding spectra are indicated in Fig. 4(*b*): DATA4, squares; DATA5, circles; DATA6, triangles. § Data were collected at beam station ID09, ESRF with X-rays of 0.75 Å wavelength. ¶ $R_{\rm merge} = \sum_i |I_i - \langle I\rangle| / \sum \langle I_i\rangle$, where I_i is the observed intensity and $\langle I_i\rangle$ is the average intensity over symmetry-equivalent measurements. †† $R = \sum ||F_{\rm obs}| - |F_{\rm calc}|| / \sum |F_{\rm obs}|$. $R_{\rm free}$ is the same as R, but for a 5% subset of all reflections that were never used in crystallographic refinement. ‡‡ One additional PO_4^{3-} molecule was placed in this model close to the surface of the protein (not in the 8-HDF pocket).

involves the absorption of a photon by the second chromophore (8-HDF or MTHF) and energy transfer from the second chromophore to $FADH^-$. This is followed by electron transfer to the pyrimidine dimer, which results in monomerization and, finally, back electron transfer, restoring the catalytically active flavin (Yasui & Eker, 1999; Sancar, 2003).

The second photochemical reaction is the photoreduction of the semi-reduced $FADH^{\cdot}$ chromophore to $FADH^-$, also referred to as photoactivation, as DNA photolyase is only active with the FAD chromophore in the fully reduced form. This reaction can be monitored by the decrease of the low-intensity band of the neutral semiquinone form ($FADH^{\cdot}$) above 500 nm, with maxima at 588 and 634 nm. Time-resolved absorption spectroscopy on *Anacystis nidulans* DNA apophotolyase showed that the light-induced reduction of the $FADH^{\cdot}$ form is associated with the formation of at least two short-lived amino-acid radicals in the protein (Aubert *et al.*, 1999). Both amino-acid radicals can decay by relatively slow charge recombination with $FADH^-$; however, in the presence of an external electron donor this recombination does not occur and the enzyme is left in its active fully reduced state. The amino-acid radicals involved in these electron-transfer reactions have been attributed as tryptophan and tyrosine residues from their respective transient absorption spectra, but they have not yet been assigned to any specific amino-acid residue in the protein.

The crystal structures of the DNA photolyases from *Escherichia coli*, *A. nidulans* and *Thermus thermophilus* have been solved at atomic resolution, indicating an N-terminal α/β dinucleotide-binding domain and a C-terminal helical domain (Park *et al.*, 1995; Tamada *et al.*, 1997; Komori *et al.*, 2001). Here, the crystallization and structure of *A. nidulans* apophotolayse as well as the holoprotein reconstitution from the apoprotein and 8-HDF are reported for the first time. In addition, studies on the effect of X-ray exposure on the redox state of the FAD chromophore in photolyase crystals during data collection at 100 K were carried out. The absorption and the structural changes calculated from three successively collected data sets were monitored, showing sub-ångström conformational changes in and around the flavin group of DNA photolyase.

2. Materials and methods

2.1. Purification and crystallization of photolyase

Recombinant DNA photolyase from the cyanobacterium *A. nidulans* was overexpressed and purified from *E. coli* as described previously (Miki *et al.*, 1993). As *E. coli* cells are unable to synthesize 8-HDF, purification results in apophotolyase containing the FAD chromophore only. Reconstitution of apophotolyase was studied using synthetic 8-hydroxy-5-deazariboflavin (Eker *et al.*, 1989). The isolation and purification of holophotolyase from *A. nidulans* cells has been described elsewhere (Eker *et al.*, 1990). For crystallization, apophotolyase was concentrated to 30 mg ml^{-1} in 10% ammmonium sulfate, 10 m*M* potassium sulfate pH 7.0 and 5 m*M* 2-mercaptoethanol by the use of a Centricon centrifugal filter device (Millipore) with a 30 kDa cutoff. Subsequently, protein crystals were obtained by the hanging-drop vapour-diffusion method: the sample was equilibrated at 277 K against the same buffer containing 22% ammonium sulfate as described elsewhere (Miki *et al.*, 1993). Crystals were frozen in liquid nitrogen after bathing at 277 K in a cryo-

protectant consisting of the precipitant containing 10%(*v*/*v*) and subsequently 30%(*v*/*v*) glycerol for a few seconds.

2.2. X-ray crystallographic analysis

A 1.8 Å resolution data set was collected from DNA apophotolyase (DATA7) at 100 K at the European Synchrotron Radiation Facility (ESRF), using the monochromatic mode (0.75 Å) at beam station ID09 (Wulff *et al.*, 1997). Further X-ray diffraction studies (DATA1–6) were carried out using synchrotron radiation with a typical dose of 8×10^{10} photons s^{-1} at the bending-magnet beamline BL44B2, SPring-8, Japan (Adachi *et al.*, 2001). Data were collected with a MAR CCD165 area detector using monochromatic X-rays of 1.00 Å. The crystals belong to the tetragonal space group $P4_32_12$, with unit-cell parameters $a = b = 90.01$, $c = 134.78$ Å. Diffraction data sets of apophotolyase (DATA1–3) and apophotolyase devoid of the semiquinone form of FAD (DATA4–6) were collected at 100 K from a single crystal. An angular range of 60 images was used with a 1.0° oscillation angle and an exposure time of 10 s, except for DATA3 and DATA6, which had a 20 s exposure time. Data sets were processed with *HKL*2000 (Otwinowski & Minor, 1997) and *CCP*4 software (Collaborative Computational Project, Number 4, 1994). Molecular replacement and rigid-body refinement were carried out using the program *CNS* (Brünger *et al.*, 1998). The atomic coordinates of the DNA holophotolyase from *A. nidulans* (PDB code 1qnf) were used as a model. Further structure refinement with *CNS* included the simulated-annealing protocol and individual *B*-factor refinement. The data-collection and refinement statistics are shown in Table 1. The root-mean-square deviation (r.m.s.d.) between DNA apophotolyase (DATA7) and holophotolyase (1qnf) was calculated using the program *LSQMAN* (Kleywegt & Jones, 1994).

2.3. Reconstitution of photolyase

DNA apophotolyase was incubated with excess 8-hydroxy-5-deazariboflavin for 4 h at 277 K and separated from unbound chromophore on a size-exclusion spin column (Bio-Spin 6, Bio-Rad) in order to obtain the absorption spectrum of reconstituted photolyase. The ratio of photolyase-bound chromophores was calculated from the absorption spectrum after heat denaturation for 10 min at 343 K followed by centrifugation.

The kinetics of reconstitution were determined by measuring the quenching of chromophore fluorescence on binding to apophotolyase,

$$\mathrm{E} + \mathrm{C} \underset{k_2}{\overset{k_1}{\rightleftharpoons}} \mathrm{EC}, \qquad (1)$$

E is apophotolyase, C is free chromophore and EC is reconstituted photolyase. In order to simplify the kinetic equation describing equilibrium (1) an at least 30-fold molar excess of apophotolyase was used, yielding

$$[\mathrm{C}] = [\mathrm{C}]_0(k_2 + k_1[\mathrm{E}]_0)\exp[-(k_2 + k_1[\mathrm{E}]_0)t]/(k_2 + k_1[\mathrm{E}]_0), \quad (2)$$

$[\mathrm{C}]_0$ and $[\mathrm{E}]_0$ are the concentrations at time $t = 0$. [C] and $[\mathrm{C}]_0$ were measured as the fluorescence intensity. Kinetic data were fitted to (2) by non-linear regression, yielding values for k_1 and k_2 and the complex association constant $K_a = k_1/k_2$. Fluorescence spectra and time courses were measured with a LS50B (Perkin–Elmer) luminescence spectrometer at 283 K.

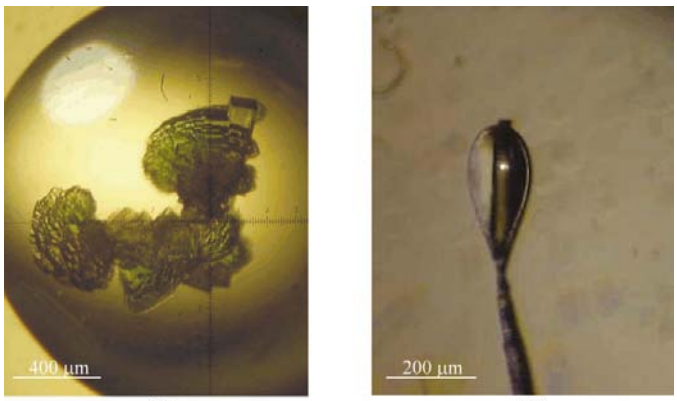

Figure 1
A. nidulans DNA photolyase crystals. (*a*) An assembly of *A. nidulans* DNA apophotolyase crystals grown after one week of incubation at 277 K and (*b*) a single $P4_32_12$ crystal isolated from the assembly and frozen in a cryoloop at 100 K in the presence of precipitant containing 30%(*v*/*v*) glycerol. The white spot on the crystal arises from the light beam of the spectrophotometer during monitoring. The dimensions of the crystal are approximately 50 × 50 × 250 µm.

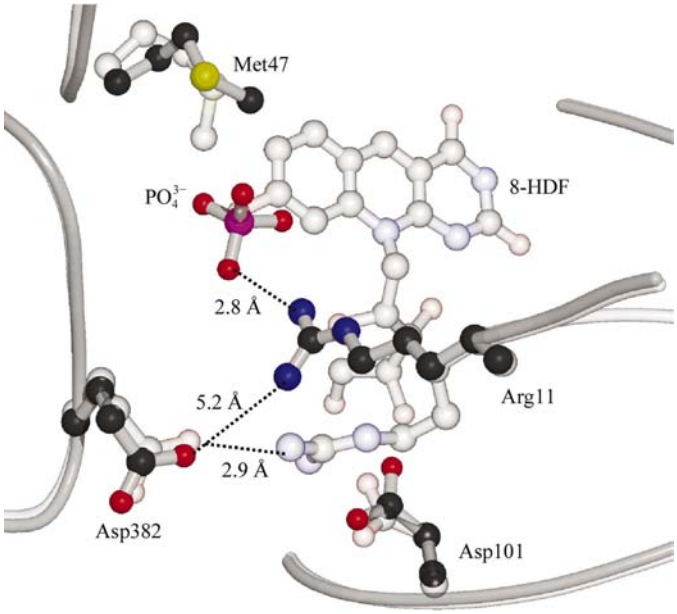

Figure 2
The 8-HDF chromophore-binding pocket in holophotolyase and apophotolyase. Residues with a significantly changed conformation in apophotolyase are depicted as a ball-and-stick model in black (C atoms), blue (N atoms), red (O atoms) and yellow (S atom). The dense colours indicate the apoprotein and the light colours the holoprotein with the 8-HDF chromophore. The additional phosphate molecule in apophotolyase is depicted in purple (P atom) and red (O atoms). The backbone is depicted as a grey wireframe.

2.4. Light-induced reduction of crystals

DNA apophotolyase crystals were mounted from the precipitant containing 30%(*v*/*v*) glycerol in a cryoloop on the goniometer head of the spectrophotometer. Crystals were illuminated for 2 s at 293 K with 20 mW helium–neon CW laser light at 633 nm (NEC Corporation, Tokyo, Japan), which was guided to the crystal by an optical fibre and a goniometer head with an adjustable fibre holder. The power density of the red laser light at the site of the sample was approximately 4 W cm^{-2}. A 600 series Oxford Cryosystems nitrogen-stream cooler was used to cool the crystal to 100 K directly after illumination. The spectra presented in Fig. 4(*a*) were recorded with a PC2000 2048-element linear CCD-array fibre-optic spectrometer (Oceanoptics Inc., Dunedin, USA). Monitoring light was focused on the crystal by the use of two reflective objectives (focal spot diameter < 50 µm). For a detailed description of this spectrophotometer, see Bourgeois *et al.* (2002).

2.5. X-ray-induced reduction of crystals

Crystals were irradiated by X-rays at 100 K using a monochromatic beam of 1.00 Å wavelength. The typical X-ray dose at the sample position at BL44B2 was 8×10^{10} photons s^{-1}. The diameter of the focused beam at the sample position is 0.22 mm, leading to a photon flux of 2×10^{12} photons mm^2 s^{-1}. Accordingly, one DNA apophotolyase crystal and one apophotolyase crystal devoid of the semiquinone form of FAD were exposed to X-ray doses of 1.2×10^{15} photons mm^{-2} (DATA1 and DATA4), 2.4×10^{15} photons mm^{-2} (DATA2 and DATA5) and 4.8×10^{15} photons mm^{-2} (DATA3 and DATA6). The absorption spectra were recorded online at SPring-8 prior to the collection of each X-ray diffraction data set. These spectra were corrected for light scattering by λ^n correction (Jagger, 1967). During the transfer between microspectrophotometer and diffractometer, crystals were kept at liquid-nitrogen temperature. As a control experiment, crystals were reduced chemically by soaking for 10 s in precipitant in the presence of 100 m*M* of the reducing agent sodium dithionite. The basic setup for the spectrophotometer used to generate the spectra has been reported by Sakai *et al.* (2002). In this study, the monochrome monitoring light was replaced by white light from a tungsten lamp to measure the full spectra and focused at the sample position to a spot diameter of 100 µm.

3. Results

3.1. Crystallization of DNA apophotolyase

Crystals of DNA apophotolyase formed large assemblies after incubation for one week at 277 K (Fig. 1*a*). The crystals belong to the tetragonal space group $P4_32_12$, with unit-cell parameters $a = b = 90.01$, $c = 134.78$ Å. These values differ only slightly from those observed for the holoprotein $P4_32_12$ crystals at room temperature ($a = b = 91.71$, $c = 135.54$ Å; Miki *et al.*, 1993). The dimensions of the single crystals that were isolated from the assemblies for spectroscopy and X-ray diffraction studies were approximately 50 × 50 × 250 µm (Fig. 1*b*). In spite of the presence of the reducing agent 2-mercaptoethanol in the initial precipitation mixture, slow oxidation of the flavin chromophore occurred, resulting in a colour change of the crystals from blue to green. Therefore, the crystallized photolyase contains both the oxidized and semi-reduced form of FAD, as is evident from the reference absorption spectrum in Fig. 4(*a*). The oxidized form of FAD exhibits characteristic absorption bands at 364 nm (not shown) and 448 nm, with the 448 nm band having fine structure at 428 and 474 nm. This spectral structure, which is also evident at room temperature, becomes more highly resolved at low temperature. In addition, the shoulder in the absorption at 498 nm and the maxima at 585 and 634 nm indicate the presence of the semi-reduced form of FAD (Eker *et al.*, 1990).

3.2. Structure of DNA apophotolyase at 1.8 Å resolution

The refined atomic structure appeared to be similar to that of the holoprotein (Tamada *et al.*, 1997), indicating that the presence of the 8-HDF chromophore is not essential for correct folding of the protein. The root-mean-square deviation over 473 C^α atoms between DNA apophotolyase (DATA7) and holophotolyase is 0.39 Å. The most striking differences in conformation were found at the 8-HDF-binding site (Fig. 2). An additional phosphate ion is present in the empty 8-HDF-binding pocket. The side chain of the Arg11 residue moves away from Asp382 by a distance of approximately 4 Å into the pocket, where it tightly interacts with the phosphate ion (2.8 Å distance). In addition to the conformational change of Arg11, slight rearrangements were observed in the side chains of Met47, Asp101 and Asp382, as depicted in Fig. 2. In addition, the conformation of Trp286 varied considerably between different DNA apophotolyase crystals (data not shown). This residue, which is highly conserved among DNA photolyases, is located at the solvent-accessible surface near the active site and its conformational flexibility is thought to be of importance for creating the cavity for pyrimidine-dimer binding for access to the FAD chromophore (Komori *et al.*, 2001).

3.3. Reconstitution of DNA photolyase

Photolyase purified from *A. nidulans* cells contains 8-hydroxy-5-deazariboflavin and FAD chromophores in a molar ratio of 1.0 (Eker *et al.*, 1990), but is hardly fluorescent. Denaturation increases the fluorescence intensity approximately 25-fold owing to the strong fluorescence of the released 8-hydroxy-5-deazariboflavin chromophore, which is quenched when bound to photolyase (Fig. 3*a*). This offers the possibility of studying the kinetics of reconstitution by measuring the decrease in fluorescence as a function of time after mixing 8-hydroxy-5-deazariboflavin with apophotolyase (Fig. 3*b*). A rather slow but almost complete quenching of fluorescence was found. Fitting the time course of the fluorescence decrease into (2) (see §2.3) yielded the kinetic constants for the reconstitution process: $k_1 = 5.8 \times 10^3\ M^{-1}\ s^{-1}$ and $k_2 = 1.5 \times 10^{-4}\ s^{-1}$ yielding the complex association constant $K_a = 4 \times 10^7\ M^{-1}$.

The absorption spectrum of apophotolyase shows only low absorption of the FAD semiquinone radical, but after reconstitution with excess 8-hydroxy-5-deazariboflavin a large absorption band (λ_{max} = 436 nm, ε_{max} = 53 000 M^{-1} cm^{-1}) is present, indistinguishable from the absorption spectrum of photolyase obtained from *A. nidulans* cells (Fig. 3*c*). From the absorption spectrum of denatured reconstituted photolyase, a molar ratio of 8-hydroxy-5-deazariboflavin:FAD of 1.1 was obtained. These results show that the presence of the Arg11 side chain and a phosphate ion the 8-HDF pocket in *A. nidulans* apophotolyase does not hamper efficient reconstitution with its natural chromophore 8-hydroxy-5-deazariboflavin.

3.4. Photoreduction of DNA apophotolyase crystals

Photoreduction of apophotolyase was studied in crystalline DNA apophotolyase. In this experiment, a crystal was cooled to 100 K in the presence of 2-mercaptoethanol as an external electron donor and the dark spectrum was measured (Fig. 4*a*). Illumination with red laser light of 633 nm under these conditions did not lead to any change in the absorption spectrum. This is in accordance with the finding that in solution the light-induced accumulation of $FADH^-$ does not occur in *A. nidulans* photolyase at temperatures below 230 K (C. Aubert and P. Mathis, personal communication), possibly owing to the temperature-dependence of the reaction with the exogenous electron donor 2-mercaptoethanol. However, red-light illumination of the crystal at room temperature for 2 s, followed by freezing to 100 K, led to a decrease in absorption in the 440–660 nm region (Fig. 4*a*). These changes indicate the light-induced conversion of the neutral semiquinone form $FADH^{\cdot}$ with absorption maxima at 498, 485 and 634 nm to the fully reduced form $FADH^-$, while photoreduction of the oxidized form FAD is virtually absent.

3.5. Structure and absorption changes by X-ray-induced FAD reduction

The absorption spectra of DNA apophotolyase crystals indicated that the absorption in the 400–700 nm region slowly decreases upon exposure to X-rays. To study the conformational changes associated with these spectral changes, three independent X-ray diffraction data sets were collected from two crystals. In addition, the corresponding absorption spectra were recorded on these two crystals prior to the collection of each data set. One crystal contained the FAD chromophore in the FADox and the $FADH^{\cdot}$ form (Fig. 4*c*) and one crystal was devoid of chromophore in the $FADH^{\cdot}$ form (Fig. 4*d*). Exposure of these two crystals to X-rays clearly shows a dose-dependent decrease of the absorption bands of FADox (Figs. 4*c* and 4*d*) as well as $FADH^{\cdot}$ (Fig. 4*c*). As a control experiment, a separate crystal was incubated in mother liquor

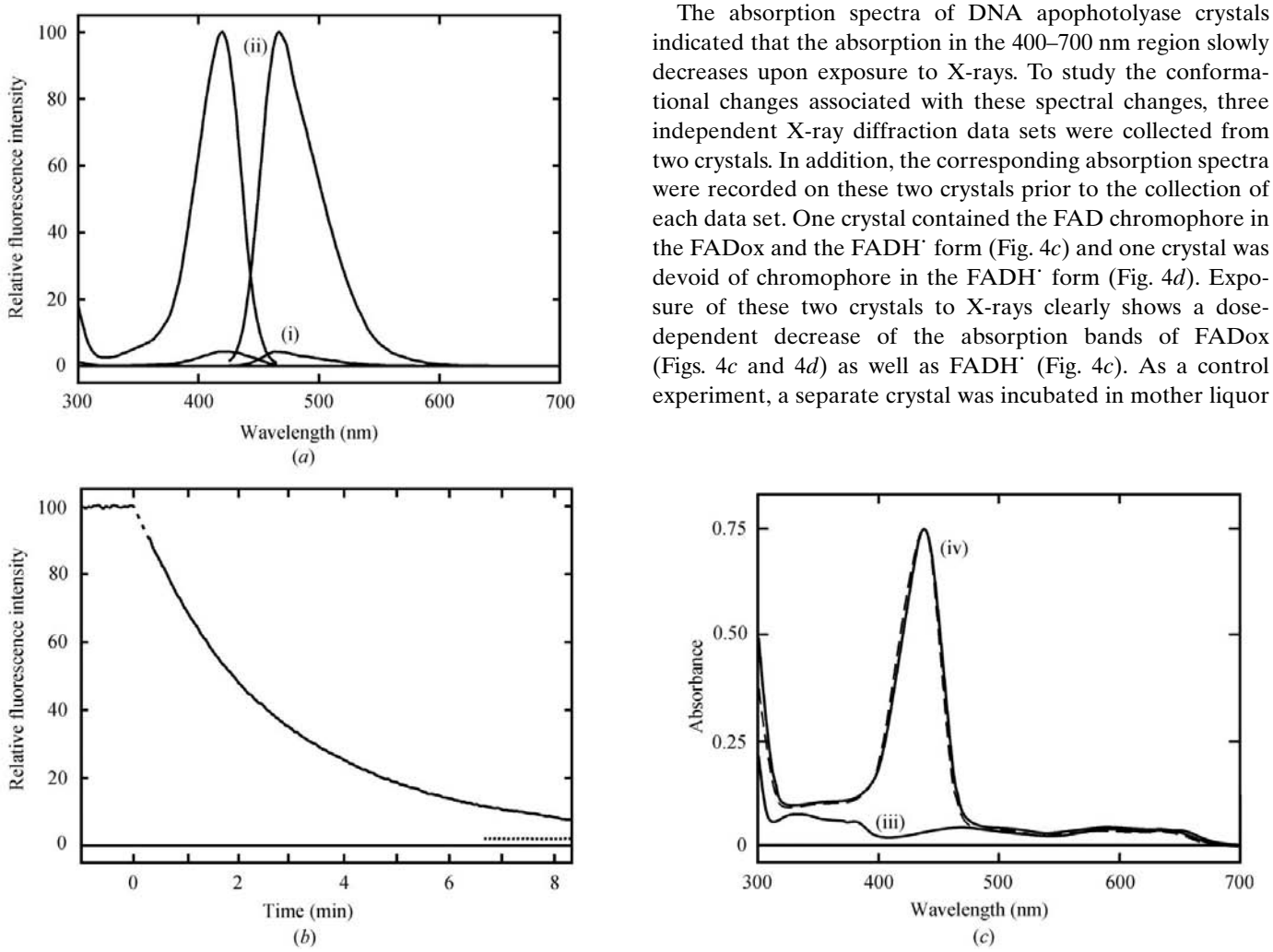

Figure 3
In vitro reconstitution of apophotolyase. (*a*) Fluorescence spectra of native (i) and heat-denatured (ii) authentic *A. nidulans* photolyase. Excitation and emission were at 420 and 468 nm, respectively. (*b*) Time course of fluorescence quenching owing to reconstitution of 8-hydroxy-5-deazariboflavin (6 n*M*) and apophotolyase (1027 n*M*) added at time zero. Excitation was at 420 nm and emission at 468 nm. The final fluorescence reached after ∼2.5 h is also shown (dotted line). (*c*) Absorption spectra of recombinant *A. nidulans* apophotolyase before (iii) and after (iv) reconstitution with 8-hydroxy-5-deazariboflavin. The absorption spectrum of authentic *A. nidulans* photolyase isolated from *A. nidulans* cells (dashed line) is shown for comparison.

with the reducing agent sodium dithionite in order to check the effect of chemical reduction on the absorption spectrum. The spectrum of a chemically reduced DNA apophotolyase crystal (Fig. 4*b*) shows similar spectral changes compared with the reference spectrum as those observed upon exposure to X-rays (Figs. 4*c* and 4*d*). They include the reduction of FADox, evident from the decrease of the 448 nm absorption band, as well as the reduction of $FADH^{\cdot}$, indicated by the decrease of absorption in the 490–660 nm region (Fig. 4*b*). Prolonged incubation in the presence of sodium dithionite further reduced the remaining oxidized form of FAD in the crystal (data not shown).

Conformational changes associated with the X-ray-induced reduction of the FAD chromophore in DNA apophotolyase at 100 K were revealed by comparison of data sets collected from a single crystal. Although differences could not be identified directly in the refined atomic models, comparison of electron-density maps of the crystal before and after X-ray irradiation by means of difference Fourier maps show significant peaks that are confined to the FAD-binding site in DNA apophotolyase (Figs. 5*a* and 5*b*). These electron-density difference peaks are shown in more detail in Figs. 5(*c*) and 5(*d*), in which the FAD-binding site of the protein has been displayed. Three combinations of negative and positive electron-density peaks are present in both maps, indicating that they are associated with the conversion of FADox to the fully reduced state. They include a number of slight displacements of approximately 0.2 Å in the structural models for the O(2) and the N(5) atom of FAD, as well as for the O^{δ} atom of Asn386, which moves toward the N(5) atom. In addition, the reduction of the $FADH^{\cdot}$ form, indicated by features that are exclusively present in Fig. 5(*c*), leads to a displacement in the refined model of 0.2 Å for the O^{δ} atom of Asp380 , which moves away from the N(3) atom in the isoalloxazine ring of FAD.

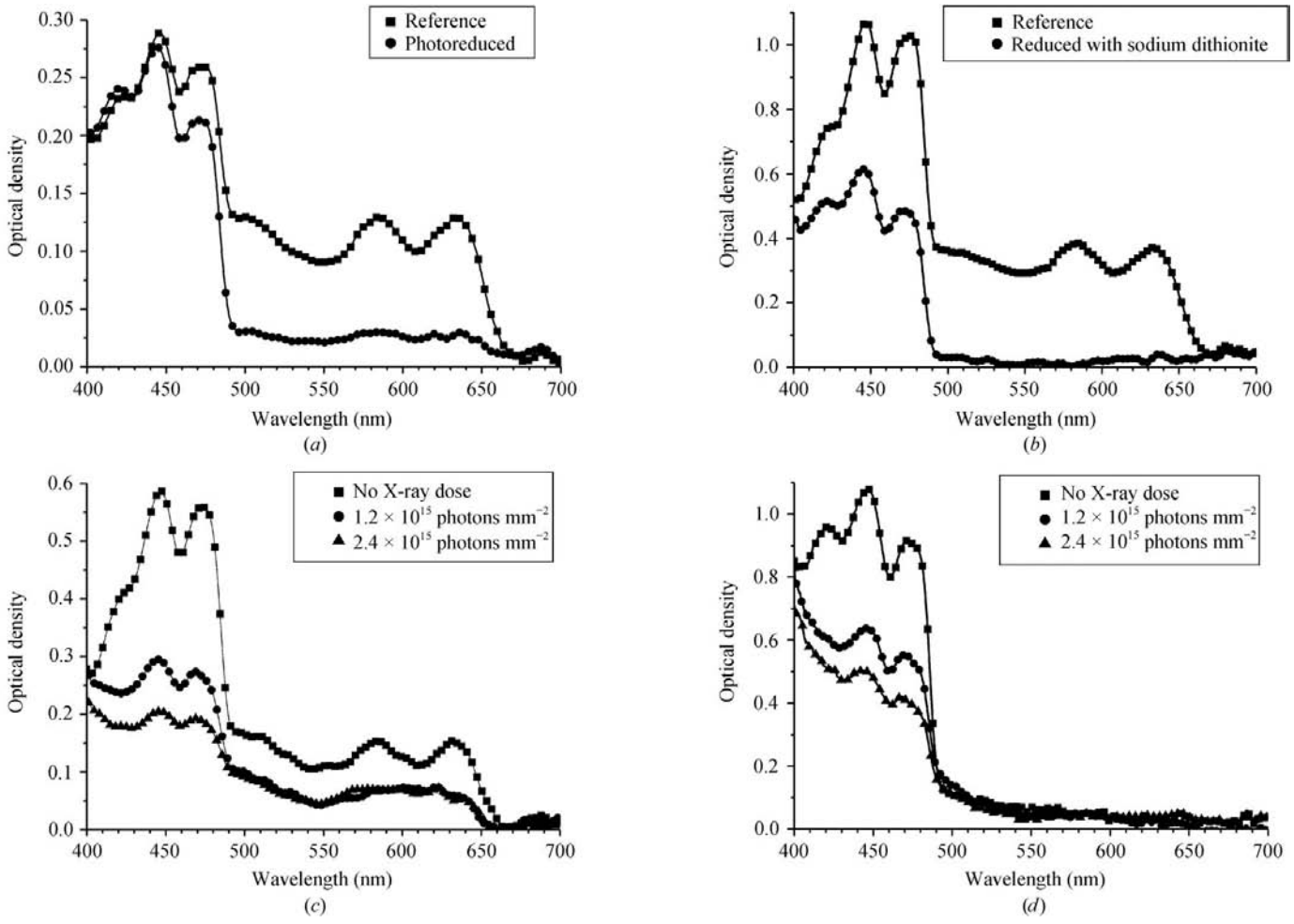

Figure 4
Reduction of crystals by light, dithionite and X-rays. (*a*) Photoreduction: light-absorption spectra were recorded at 100 K before (squares) and after (circles) illumination with 633 m He–Ne laser light for 2 s at 293 K. (*b*) Chemical reduction: spectra were recorded at 100 K without (squares) and after (circles) incubation of a crystal for 10 s at 293 K in mother liquor with 100 m*M* sodium dithionite. (*c*) X-ray-induced reduction of an apophotolyase crystal with the chromophore in the FADox and $FADH^{\cdot}$ states. Spectra were recorded on the same crystal before collection of diffraction data sets DATA1 (squares), DATA2 (circles) and DATA3 (triangles). The latter two spectra were corrected for light scatter. (*d*) X-ray-induced reduction of an apophotolyase crystal devoid of the semiquinone form of the FAD chromophore. Spectra were recorded on the same crystal before collection of diffraction data sets DATA4 (squares), DATA5 (circles) and DATA6 (triangles). The latter two spectra were corrected for light scatter. Only one out of every ten data points has been displayed in all spectra for reasons of clarity.

4. Discussion

In this study, we describe the crystallization of DNA apophotolyase, which appeared to crystallize under very similar conditions and in the same symmetry group as the holoprotein (Miki *et al.*, 1993). In line with this, differences in the apoprotein crystal structure are confined to the 8-HDF pocket. These findings show that the presence of the 8-HDF chromophore is not a prerequisite for correct folding of the protein. This is an important validation of the relevance of the observed intraprotein electron-transfer reactions in *A. nidulans* devoid of the 8-HDF antenna cofactor (Aubert *et al.*, 1999, 2000). Notwithstanding the structural rearrangements in the 8-HDF pocket, we showed that *in vitro* reconstitution of apophotolyase with 8-hydroxy-5-deazariboflavin is efficient, with an association constant $K_a = 4 \times 10^7\ M^{-1}$. This is an important result as it opens the possibility of studying energy transfer with modified flavins. The K_a value explains why, despite the low concentration of both apophotolyase (Eker *et al.*, 1990) and 8-hydroxy-5-deazariboflavin (Eker *et al.*, 1989), a reasonable amount of holophotolyase is found in the living cell.

In addition, this study describes the reduction of *A. nidulans* DNA apophotolyase crystals by X-rays and associated conformational changes. Initial experiments were aimed at the identification of conformational changes resulting from photoreduction of the FAD cofactor by exposure to 633 nm laser light (for spectra, see Fig. 4*a*). This type of experiment could not be carried out on a single frozen crystal, as light-induced accumulation of $FADH^-$ does not occur at low temperatures. Besides, an increase in the temperature of the nitrogen stream around the crystal for the purpose of photoreduction after X-ray diffraction data collection strongly affects the X-ray diffraction properties of the crystal. Therefore, comparison of data sets of flash-frozen crystals kept in the dark and after exposure of 633 nm light pulse for 2 s at room temperature were carried out. However, this multiple-crystal strategy did not lead to the identification of structural changes associated with photoreduction, as it was not possible to discriminate between the very small light-induced conformational changes and the differences resulting from non-isomorphism among crystal samples (evident from the disagreement between scaled data sets). In addition, the slow reduction of FADox and $FADH^{\cdot}$ induced by X-rays further complicated the correct interpretation of these data sets. Recently, Berglund and coworkers have reported an elegant method of dealing with the latter problem using a multiple-crystal data-collection strategy based on a systematic spread of the X-ray dose over many crystals (Berglund *et al.*, 2002). However, this method also requires the collection of data sets from different crystals, which appeared not to be suitable for the non-isomorphic DNA apophotolyase crystals used in this study. Therefore, the observed radiation-induced decay of FADox and $FADH^{\cdot}$ in a

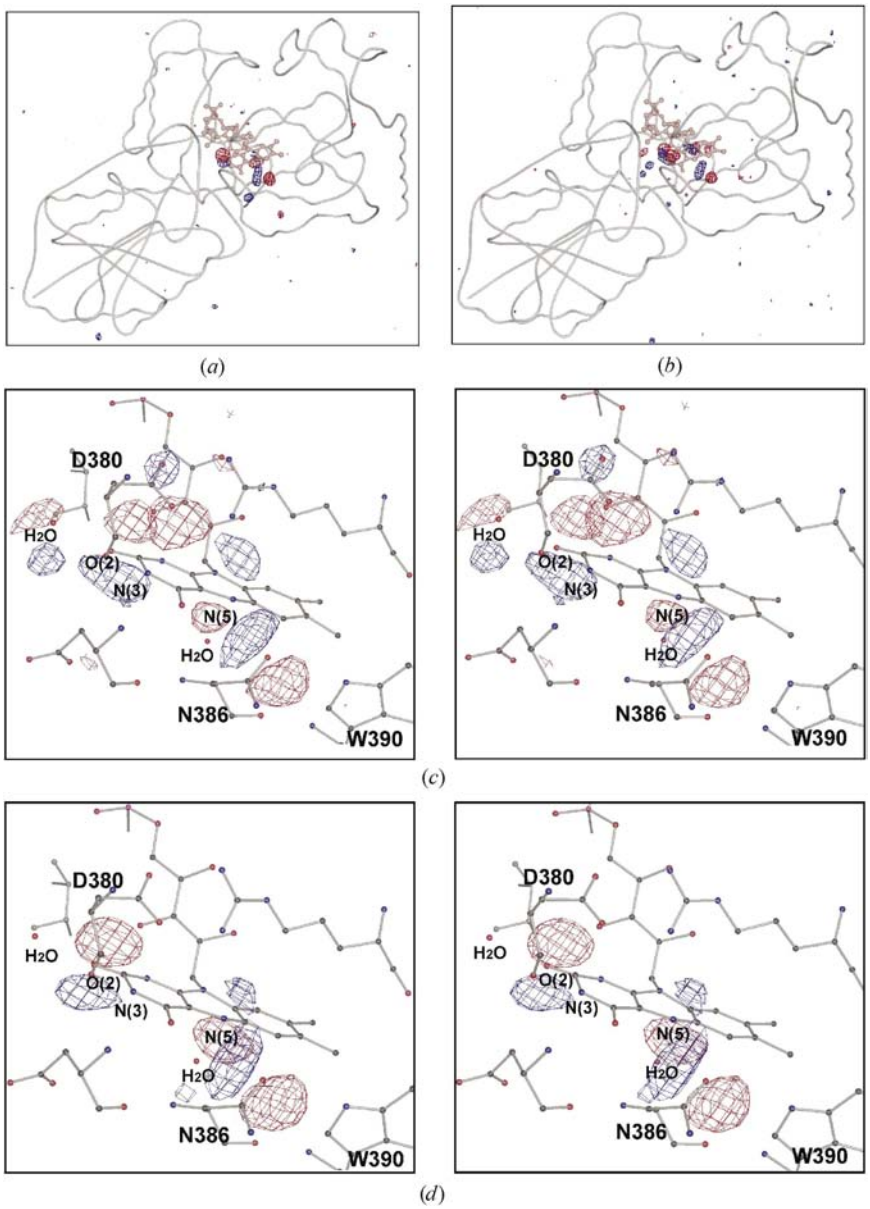

Figure 5
Structural changes upon exposure of DNA apophotolyase to X-rays. (*a*, *b*) Difference Fourier electron-density maps of the entire protein and (*c*, *d*) stereoviews of the FAD-binding site, showing the negative and positive electron-density peaks. The maps were calculated at 2.5 Å resolution. The contour levels are -4.0σ (red) and 4.0σ (blue). The figures were constructed with the programs *MOLSCRIPT* (Kraulis, 1991), *RASTER3D* (Merritt & Murphy, 1994) and *CONSCRIPT* (Lawrence & Bourke, 2000). (*a*) and (*c*) indicate difference maps calculated with structure-factor amplitudes $F_{DATA3} - F_{DATA1}$ (Table 1). (*b*) and (*d*) indicate difference maps of a crystal devoid of the semiquinone form of FAD with amplitudes $F_{DATA6} - F_{DATA4}$. See Fig. 4 for the corresponding absorption spectra and X-ray doses.

single crystal at low temperatures was used here to elucidate the structural changes associated with changes in the redox state of the FAD cofactor of DNA photolyase. The observed decay of these redox states as indicated in Figs. 4(*c*) and 4(*d*) was interpreted as a result of reduction. This interpretation was further substantiated by incubation of crystals in the presence of the reducing agent sodium dithionite, which led to similar changes in the absorption properties of DNA apophotolyase crystals (Fig. 4*b*). The reduction of a redox-active group in a protein crystal by X-rays at cryogenic temperatures and associated structural changes have also been observed in a number of metalloproteins (Chance *et al.*, 1980; Schlichting *et al.*, 2000). This effect is interpreted as a reduction by radiolytically produced electrons, derived from the solvent for example, that drive the reaction. Radiolysis from X-rays has been reported to cause specific structural changes, including the breakage of disulfide bridges and the decarboxylation of acidic residues (Burmeister, 2000; Weik *et al.*, 2000).

Irradiation of DNA apophotolyase crystals at low temperature led to a number of interesting structural changes that can be observed as combinations of negative and positive density in the Fourier difference maps (Fig. 5). The conversion of FADox to its fully reduced form leads to a slight movement of O(2) relative to the isoalloxazine ring and a possibly correlated movement of the O^{δ} atom of Asn386 and the N(5) atom in the isoalloxazine ring. More extensive movements in the isoalloxazine ring of FAD have been reported for thioredoxin reductase (Lennon *et al.*, 1999). In this enzyme the ring is planar in the oxidized form, but makes a 34° 'butterfly bend' about the N(5)—N(10) axis in the reduced form. The strengthening of a hydrogen bond with N(5) upon reduction is a common phenomenon in flavoproteins and plays a role in the stabilization of reduced FAD. For example, in flavodoxins it has been observed that reduction of the flavin mononucleotide group is associated with the flipping of a Gly-Asp dipeptide in the protein, where the carbonyl oxygen of the Gly accepts a hydrogen bond from N(5) in the semiquinone and hydroquinone forms (Ludwig *et al.*, 1997). In the present study it is shown that the O^{δ} atom of Asn386 moves to a slightly closer contact of 3.3 Å with the N(5) atom in the isoalloxazine ring. The O^{δ} atom of Asn386 is also in 3.4 Å contacting distance with the N^{ε} atom of Trp390, which is the homologue of Trp382 in *E. coli* photolyase, the electron donor to FAD (Byrdin *et al.*, 2003; Cheung *et al.*, 1999). It is tempting to speculate that Trp390 takes part in the so far unidentified electron-transport pathway, as the earliest amino-acid radical observed so far upon light excitation of *A. nidulans* DNA photolyase is a tryptophan radical (Aubert *et al.*, 1999). One additional set of features that can be designated to the reduction of $FADH^{\cdot}$ include the movement of the O^{δ} atom of Asp380 away from the N(3) atom in the isoalloxazine ring (Fig. 5*c*). However, at this point it is not clear whether the observed structural changes upon $FADH^{\cdot}$ reduction in DNA photolyase reflect to some extent the changes occurring during the process of photoactivation.

This work was supported by a grant from the 'Research for the Future' Program (97L00501) and a Grant-in-Aid for Scientific Research (No. 14208081) to KM, a Postdoctoral Fellowship (ID No. P 99766) to RK and a Grant-in-Aid to HK (No. 4741), all from the Japanese Society for the Promotion of Science. RK is grateful to Drs R. Ravelli, F. Schotte and M. Wulff for their support at beam station ID09, ESRF. The authors thank Drs K. J. Hellingwerf, J. H. J. Hoeijmakers, M. Kataoka and Y. Shiro for their interest in this work.

References

Adachi, S., Oguchi, T., Tanida, H., Park, S. Y., Shimizu, H., Miyatake, H., Kamiya, N., Shiro, Y., Inoue, Y., Ueki, T. & Iizuka, T. (2001). *Nucl. Instrum. Methods A*, **467**, 711–714.

Aubert, C., Mathis, P., Eker, A. P. M. & Brettel, K. (1999). *Proc. Natl Acad. Sci. USA*, **96**, 5423–5427.

Aubert, C., Vos, M. H., Mathis, P., Eker, A. P. M. & Brettel, K. (2000). *Nature (London)*, **405**, 586–590.

Berglund, G. I., Carlsson, G. H., Smith, A. T., Szoke, H., Henriksen, A. & Hajdu, J. (2002). *Nature (London)*, **417**, 463–468.

Bourgeois, D., Vernede, X., Adam, V., Fioravanti, E. & Ursby, T. (2002). *J. Appl. Cryst.* **35**, 319–326.

Brünger, A. T., Adams, P. D., Clore, G. M., DeLano, W. L., Gros, P., Grosse-Kunstleve, R. W., Jiang, J.-S., Kuszewski, J., Nilges, M., Pannu, N. S., Read, R. J., Rice, L. M., Simonson, T. & Warren, G. L. (1998). *Acta Cryst.* D**54**, 905–921.

Burmeister, W. P. (2000). *Acta Cryst.* D**56**, 328–341.

Byrdin, M., Eker, A. P., Vos, M. H. & Brettel, K. (2003). *Proc. Natl Acad. Sci. USA*, **100**, 8676–8681.

Chance, B., Angiolillo, P., Yang, E. K. & Powers, L. (1980). *FEBS Lett.* **112**, 178–182.

Cheung, M. S., Daizadeh, I., Stuchebrukhov, A. A. & Heelis, P. F. (1999). *Biophys. J.* **76**, 1241–1249.

Collaborative Computational Project, Number 4 (1994). *Acta Cryst.* D**50**, 760–763.

Eker, A. P., Hessels, J. K. & Meerwaldt, R. (1989). *Biochim. Biophys. Acta*, **990**, 80–86.

Eker, A. P., Kooiman, P., Hessels, J. K. & Yasui, A. (1990). *J. Biol. Chem.* **265**, 8009–8015.

Jagger, J. (1967). *Introduction to Research in Ultraviolet Photobiology*, p. 53. Englewood Cliffs, New Jersey, USA: Prentice Hall Inc.

Kleywegt, G. J. & Jones, T. A. (1994). *Jnt CCP4–ESF/EACBM Newsl. Protein Crystallogr.* **31**, 9–14.

Komori, H., Masui, R., Kuramitsu, S., Yokoyama, S., Shibata, T., Inoue, Y. & Miki, K. (2001). *Proc. Natl Acad. Sci. USA*, **98**, 13560–13565.

Kraulis, P. J. (1991). *J. Appl. Cryst.* **24**, 946–950.

Lawrence, M. C. & Bourke, P. (2000). *J. Appl. Cryst.* **33**, 990–991.

Lennon, B. W., Williams, C. H. & Ludwig, M. L. (1999). *Protein Sci.* **8**, 2366–2379.

Ludwig, M. L., Pattridge, K. A., Metzger, A. L., Dixon, M. M., Eren, M., Feng, Y. C. & Swenson, R. P. (1997). *Biochemistry*, **36**, 1259–1280.

Merritt, E. A. & Murphy, M. E. P. (1994). *Acta Cryst.* D**50**, 869–873.

Miki, K., Tamada, T., Nishida, H., Inaka, K., Yasui, A., de Ruiter, P. E. & Eker, A. P. (1993). *J. Mol. Biol.* **233**, 167–169.

Otwinowski, Z. & Minor, W. (1997). *Methods Enzymol.* **276**, 307–326.

Park, H. W., Kim, S. T., Sancar, A. & Deisenhofer, J. (1995). *Science*, **268**, 1866–1872.

Sakai, K., Matsui, Y., Kouyama, T., Shiro, Y. & Adachi, S. (2002). *J. Appl. Cryst.* **35**, 270–273.

Sancar, A. (2003). *Chem. Rev.* **103**, 2203–2237.

Schlichting, I., Berendzen, J., Chu, K., Stock, A. M., Maves, S. A., Benson, D. E., Sweet, B. M., Ringe, D., Petsko, G. A. & Sligar, S. G. (2000). *Science*, **287**, 1615–1622.
Tamada, T., Kitadokoro, K., Higuchi, Y., Inaka, K., Yasui, A., de Ruiter, P. E., Eker, A. P. M. & Miki, K. (1997). *Nature Struct. Biol.* **4**, 887–891.
Weik, M., Ravelli, R. B. G., Kryger, G., McSweeney, S., Raves, M. L., Harel, M., Gros, P., Silman, I., Kroon, J. & Sussman, J. L. (2000). *Proc. Natl Acad. Sci. USA*, **97**, 623–628.
Wulff, M., Schotte, F., Naylor, G., Bourgeois, D., Moffat, K. & Mourou, G. (1997). *Nucl. Instrum. Methods A*, **398**, 69–84.
Yasui, A. & Eker, A. P. M. (1999). *DNA Damage and Repair*, Vol. 2, edited by J. A. Nickoloff & M. F. Hoekstra, pp. 9–32. Totowa, New Jersey, USA: Humana Press Inc.